Metal Chains

DOI: 10.1002/ange.200501049

Paramagnetic Platinum–Rhodium Octamers Bridged by Halogen Ions To Afford a Quasi-1D System**

Kazuhiro Uemura, Kôichi Fukui, Hiroyuki Nishikawa, Saiko Arai, Kazuko Matsumoto, and Hiroki Oshio*

One-dimensional (1D) materials have long fascinated physicists and chemists because of their unusual physical properties.[1,2] It has been recognized that stacks of mixed-valent organic and inorganic molecules exhibit unusual electrical properties owing to the alternate donor–acceptor interactions within the stack column, as found in [(TTF)(TCNQ)] (TTF = tetrathiafulvalene, TCNQ = tetracyanoquinodimethane), square-planar $[Pt(CN)_4]^{n-}$, and $K_2[Pt(CN)_4]X_{0.3}$ (X = Cl, Br).[3] The future goal in this area is to prepare "synthetic metals" and establish the superconducting state in low-dimensional materials.[2] To rationally synthesize 1D chains of conducting materials, a judicious choice of mixed-valent metal complexes (Pt, Rh, etc.) is necessary.[4] "Platinum blue" has a linear tetranuclear metal–metal bonded backbone with mixed valency $(Pt^{2.25+})_4$, and the one unpaired electron of the complex is delocalized over the four platinum centers,[5,6] whose redox properties based on $Pt^{III/II}$ have been well-studied and applied to catalysis.[5] Introduction of this fascinating structure into 1D conducting materials has, to our knowledge, not been attempted. Herein, we report the

[*] Dr. K. Uemura, Dr. K. Fukui, S. Arai, Prof. Dr. K. Matsumoto
Department of Chemistry, School of Science and Engineering
Advanced Research Institute for Science and Engineering
Waseda University
3-4-1, Ohkubo, Shinjuku, Tokyo 169-8555 (Japan)
Fax: (+81) 3-5273-3489
E-mail: kmatsu@waseda.jp
Dr. H. Nishikawa, Prof. Dr. H. Oshio
Department of Chemistry
University of Tsukuba
Tennoudai 1-1-1, Tsukuba, Ibaraki 305-8571 (Japan)

[**] This work was partially supported by the Nano COE and the 21COE program Practical Nano-Chemistry from MEXT, Japan.

Supporting information for this article is available on the WWW under http://www.angewandte.org or from the author.

synthesis, X-ray crystal structure analysis, and magnetic properties of the infinite chain of Pt_6Rh_2 moieties bridged by Cl^- ions.

Our strategy for the synthesis of a 1D chain is to rationally align dinuclear basic units doubly bridged with amidate ligands as found in platinum blue backbones. We previously reported the synthesis and structure of $[Pt(PVM)_2(NH_3)_2]\cdot 2H_2O$ (**1**, PVM = pivalamidate),[7] which can easily bind a second metal ion with the noncoordinated oxygen atoms of the amide moieties[8] to afford various dinuclear and trinuclear Pt complexes (Scheme 1).[7] For example, a simple mixture of **1** and $RhCl_3\cdot 3H_2O$ in MeOH provides the dinuclear complex, $[PtRh(PVM)_2(NH_3)_2Cl_3]$.[9,10] Such facile dimerization is attributed to the thermal instability of **1** in the solution state which is manifested by the release of PVM upon addition of excess $NaPF_6$ to **1** in MeOH[11] to give yellow-green crystals of $[Pt_2(PVM)_2(NH_3)_4](PF_6)_2\cdot H_2O$ (**2**). The oxidized **2**—platinum blue—was synthesized from the reaction of **1** and the hydrolysis product of *cis*-$[PtCl_2(NH_3)_2]$ and was isolated as dark green $[Pt_4(PVM)_4(NH_3)_8](PF_6)_4(ClO_4)\cdot 2H_2O$ (**3**). Figure 1 shows the crystal structures of **2** and **3**. Both single crystals of **2** and **3** consist of tetranuclear platinum chains (Figure 1 a and c). It is known that tetraplatinum chain structures are achieved only with head-to-head (HH) dimers and that dimer–dimer interactions are generally stabilized by a Pt–Pt bond and/or four hydrogen bonds formed between the oxygen atoms of the amidate and the hydrogen atoms of the ammine ligands. These tetranuclear structures are essentially identical to those reported previ-

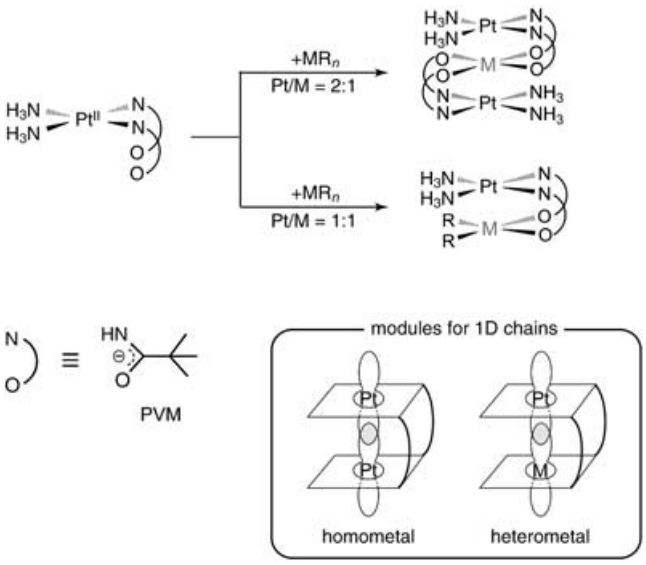

Scheme 1. Reaction scheme for $[Pt(PVM)_2(NH_3)_2]\cdot 2H_2O$ (**1**), which can easily bind a second metal ion to afford various di- and trinuclear Pt complexes as shown.

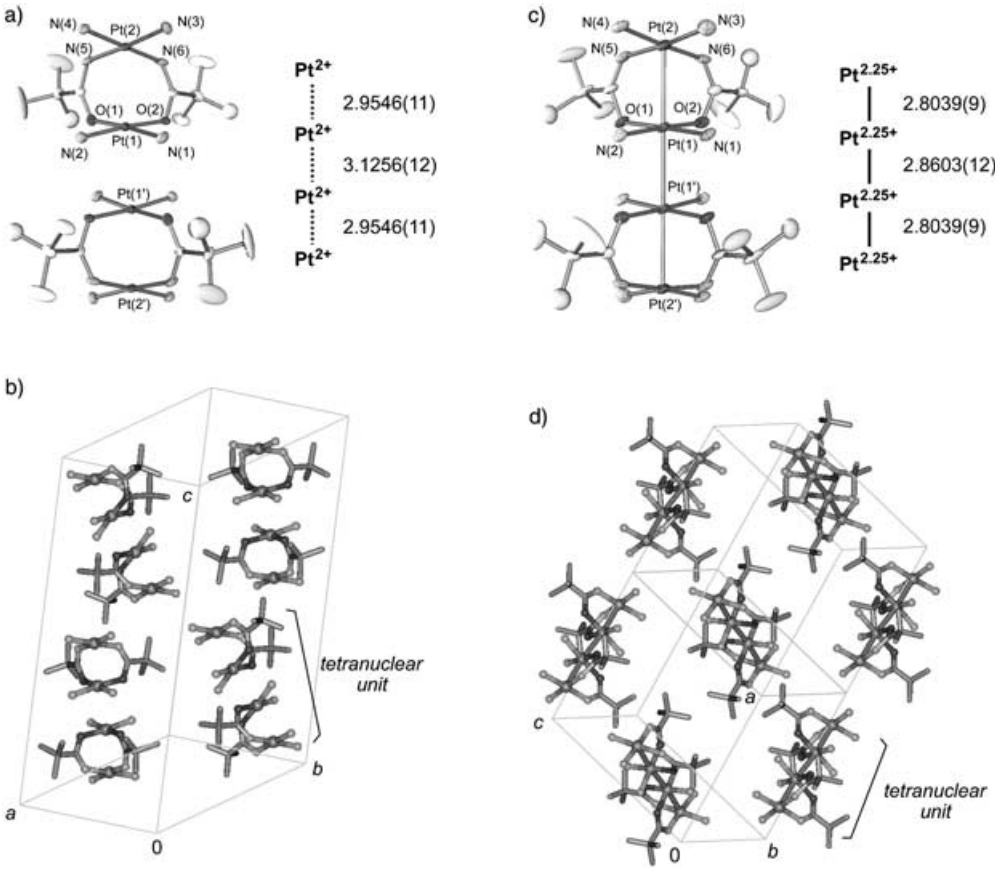

Figure 1. a) Crystal structure and b) packing diagram of $[Pt_2(PVM)_2(NH_3)_4](PF_6)_2\cdot H_2O$ (**2**), and c) crystal structure and d) packing diagram of $[Pt_4(PVM)_4(NH_3)_8](PF_6)_4(ClO_4)\cdot 2H_2O$ (**3**, platinum blue). Schematic drawings for the oxidation states of platinum atoms and metal–metal bonding lengths are also shown in (a) and (c). Hydrogen atoms, PF_6^- and ClO_4^- ions, and solvent molecules (H_2O) are omitted for clarity.

ously with other amidate ligands.[6,12,13] Each platinum atom in the dimer is *cis*-coordinated to two ammine ligands and to either two oxygen atoms or two deprotonated nitrogen atoms of the PVM ligands. X-ray diffraction analysis revealed that four PF_6^- anions are present per tetranuclear unit in **2** and **3**, with an additional ClO_4^- ion present in the latter structure, and therefore the average oxidation state of platinum in **2** and **3** is +2 and +2.25, respectively. In both crystal structures, the tetrameric platinum units are packed without significant interaction with each other (Figure 1b and 1d).

The precursors to the two complexes, dinuclear $[PtRh(PVM)_2(NH_3)_2Cl_3]$ and tetranuclear **2**, were mixed together in a vessel, and brown single crystals of $\{[PtRh(PVM)_2(NH_3)_2Cl_{2.5}]_2[Pt_2(PVM)_2(NH_3)_4]_2(PF_6)_6{\cdot}2\,MeOH{\cdot}2\,H_2O\}_n$ (**4**) with metallic luster were successfully obtained upon evaporation of the solution in air. Figure 2 shows the crystal structure of **4**. The most remarkable structural feature is that the complex cation is an infinite repetition of the octameric segment of Pt_6Rh_2 bridged by the Cl^- ion, with a crystallographic inversion center at the center of the octamer. The Pt_6Rh_2 octameric segment consists of four dimeric units (inner dimers; Pt(1)–Pt(2), Pt(1′)–Pt(2′), outer dimers; Rh(1)–Pt(3), Rh(1′)–Pt(3′)), each doubly bridged by PVM ligands. The inner tetrameric platinum unit (Pt(2)-Pt(1)-Pt(1′)-Pt(2′)) has a structure that is quite similar to those of **2** and **3**. The central interdimer interaction is reinforced by four hydrogen bonds between the oxygen atoms of PVM and the hydrogen atoms of the ammine ligands. The distance between the PVM-bridged platinum atoms (Pt(1)–Pt(2): 2.8450(7) Å) is shorter by 0.218 Å than the inner Pt(1)–Pt(1′) distance of 3.0634(10) Å. The outer dimers, $[PtRh(PVM)_2(NH_3)_2Cl_2]^{n+}$ (Pt(3)–Rh(1) 2.5987(11) Å), are bonded to both ends of the tetranuclear platinum unit at a Pt(2)–Rh(1) distance of 2.7337(11) Å and a typical torsion angle of 45°. Additionally, the Pt_6Rh_2 octameric segments are bridged by Cl^- ligands (Pt(3)–Cl(3) 2.5959(6) Å) to give a very attractive pseudo-1D infinite chain expressed as $[\text{-Pt-Rh-Pt}_4\text{-Rh-Pt-Cl-}]_n$. Three types of crystal structures based similarly on the tetrameric platinum unit have been reported to date, namely 1) the octameric platinum oligomer,[14] 2) the Cl^--bridged platinum tan[6f] like M_4X-type chain, and 3) the infinite platinum wire.[4h] In contrast, the present system is a quasi-1D system, which is distinct from the previous systems on the grounds that two kinds of metals are conjugated in the system which leads to the unique metal–metal interactions and magnetic properties observed.

Table 1 summarizes the selected bond lengths and angles of the tetrameric platinum units in **2**–**4**. Both the inter- and intradimer Pt–Pt distances in **4** are slightly longer than the corresponding lengths of **3**, but still much shorter than those in **2**. Also, the lengths of the hydrogen bonds observed between the amide oxygen and ammine nitrogen atoms in the interdimers in **4** are intermediate between the lengths of the corresponding bonds in **2** and **3**. The tilt angle (τ) between the Pt(1) and Pt(2) coordination planes increases as the Pt–Pt distance increases, as observed also in the series α-pyrrolidonate-tan,[13a] -blue,[6f] and -yellow.[12e] The charge of +19 for the Pt_6Rh_2 octameric segment in **4** was determined from the number of independent PF_6^- ions, which is exactly

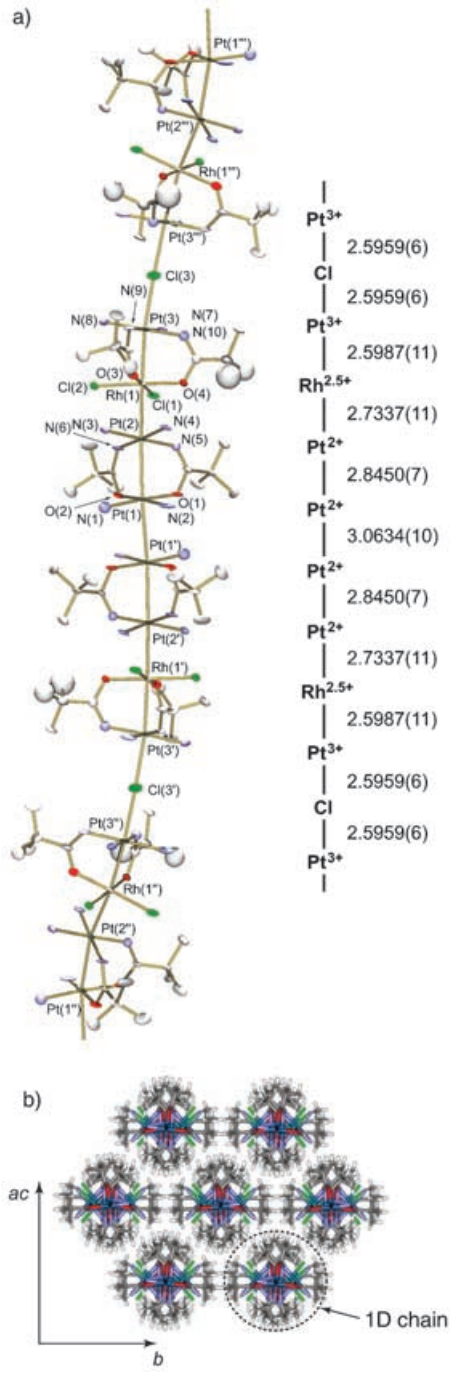

Figure 2. a) Crystal structure of $\{[PtRh(PVM)_2(NH_3)_2Cl_{2.5}]_2[Pt_2(PVM)_2(NH_3)_4]_2(PF_6)_6{\cdot}2\,MeOH{\cdot}2\,H_2O\}_n$ (**4**) with a schematic drawing of the metal–metal bond lengths (hydrogen atoms, PF_6^- ions, and solvent molecules (MeOH and H_2O) are omitted for clarity). b) Crystal packing diagram of the 1D chains in **4** (PF_6^- ions and solvent molecules (MeOH and H_2O) are omitted for clarity).

Table 1: Selected bond lengths [Å] and angles [°] for **2**, **3**, and **4**.

	2	**3**	**4**
Pt(1)–Pt(2)	2.9546(11)	2.8039(9)	2.8450(7)
Pt(1)–Pt(1′)	3.1256(12)	2.8603(12)	3.0634(10)
hydrogen bonds (NH···O)	2.96, 2.96, 2.98, 2.98	2.78, 2.78, 2.85, 2.85	2.91, 2.91, 2.91, 2.91
tilt angle (τ)	27.3	21.8	23.1

six, in the X-ray refinement of the ion occupancies. These results provide convincing evidence that the material is composed of Pt and Rh atoms with one unpaired electron per Pt_6Rh_2Cl unit. The increase in the Pt–Pt distance with a decrease in the average oxidation state of platinum is widely observed in this class of compound.[13a] Assuming this relationship holds in **4**, the average oxidation state of the inner tetrameric platinum unit in **4** appears to be between +2.0 and +2.25.

Figure 3 shows the EPR spectra of **3** in a water/ethylene glycol (1:1 v/v) glass and powder samples of **3** and **4** measured at 77 K. The EPR spectrum of **3** in the glass exhibits sharp perpendicular and parallel peaks, each split into at least nine lines due to ^{195}Pt nuclei ($I = 1/2$ with an abundance of 33.7 %). The EPR parameters have been determined by computer simulations as $g_\perp = 2.393$, $g_\parallel = 1.979$, $A_{1\perp} = 429$ MHz, $A_{1\parallel} = 499$ MHz, $A_{2\perp} = 861$ MHz, and $A_{2\parallel} = 679$ MHz. These values are similar to those reported for platinum blue.[6b,15] Powdered **3** shows a broad axial-type signal with no resolved hyperfine splittings ($g_\perp = 2.350$, $g_\parallel = 2.030$; peak-to-peak line width, $W_\perp = 12.5$ mT, $W_\parallel = 12.5$ mT), whereas the powder sample of **4** exhibits a much broader ($W = 45.0$ mT) signal centered at a smaller value of g_{av} ($g_{av} = 2.032$).

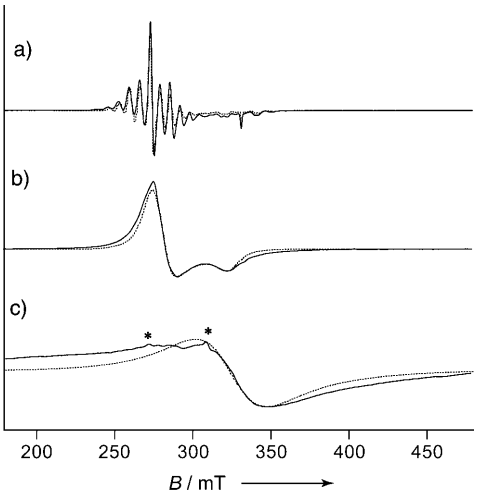

Figure 3. Continuous wave EPR spectra measured at 77 K for a) **3** in a water/ethylene glycol (1:1 v/v) glass, b) **3** (powder sample), and c) **4** (powder sample). Experimental settings: microwave frequency: 9.1826 (a), 9.2022 (b), and 9.1988 GHz (c); microwave power: 5 mW; field modulation (100 kHz): 0.1 mT. Asterisks indicate the platinum blue impurity (around 270 mT); solid lines are the measured spectra, and dotted lines are the simulations.

The *g* values obtained for **3** are well interpreted in terms of a d_{z^2}-hole state (the *z* axis lies along the mean Pt chain) with an admixture of the lower-lying d_{xz} and d_{yz} states due to spin–orbit coupling.[15] Typical examples for d_{z^2}-type Pt complexes are Pt^{IV}-doped $[Pt(NH_3)_4][PtCl_4]$ ($g_\perp = 2.504$, $g_\parallel = 1.939$, $g_{av} = 2.316$),[16] *cis*-diammineplatinum α-pyridone blue ($g_\perp = 2.381$, $g_\parallel = 1.975$, $g_{av} = 2.246$),[6b] and $[K_2Pt(CN)_4Br_{1/3}]\cdot 3H_2O$ (KCP, $g_\perp = 2.336$, $g_\parallel = 1.946$, $g_{av} = 2.206$).[17] All these values are attributed to the d_{z^2}-hole state of Pt^{III}. On the other hand, the EPR spectrum of **4** is quite different from that of **3** and features 1) a relatively small g_{av} value and 2) a broad spectrum profile. If it is taken into account that the g_{av} value of **4** ($g_{av} = 2.032$) is much smaller than those of the d_{z^2}-type Pt complexes, it is unlikely that the unpaired electron occupies the d_{z^2} state in **4**. It is important to note that the d_{z^2}-type Rh^{II} complexes exhibit a relatively large g_{av} value in similar fashion to Pt^{III} (e.g. $g_{av} = 2.176$ for [(TTiPP)Rh^{II}] (TTiPP = tetrakis(1,3,5-triisopropylphenyl)porphyrin)).[18] Considering the small g_{av} value of **4**, which is different from both Pt^{III} and Rh^{II}, the singly occupied orbital in **4** is attributed most likely to the Rh^{II} d_{xy} orbital, which is raised in energy above d_{z^2} through π interactions with the amidate ligands (Scheme 2). The broad nature of the EPR spectrum of

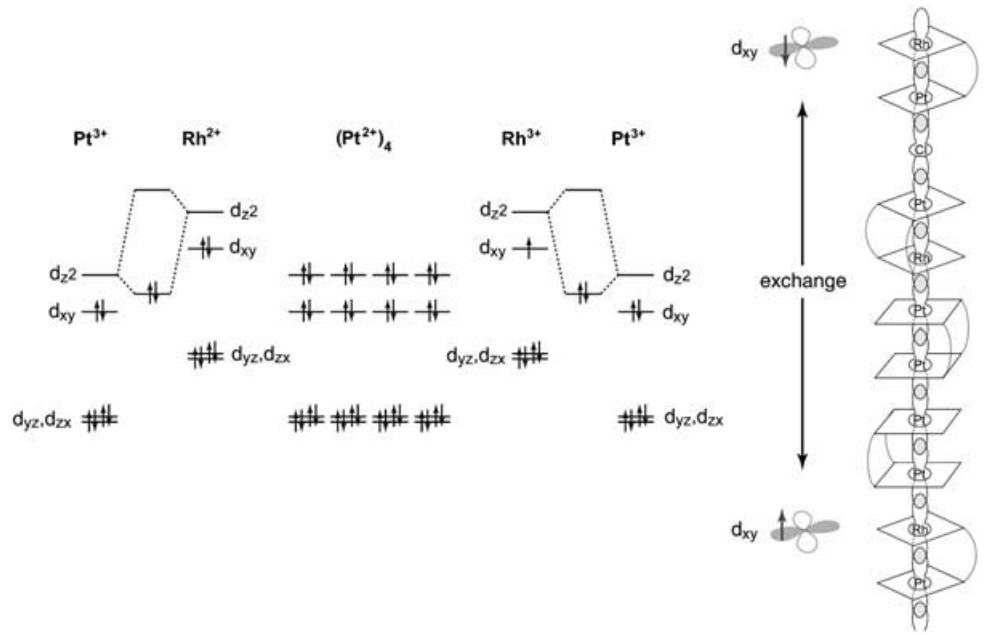

Scheme 2. Molecular orbital diagram of $\{[PtRh(PVM)_2(NH_3)_2Cl_{2.5}]_2[Pt_2(PVM)_2(NH_3)_4]_2(PF_6)_6\cdot 2\,MeOH\cdot 2H_2O\}_n$ (**4**) with schematic structural view.

4 can be attributed to a long-distance exchange interaction. The magnetic susceptibility measurement of **4** shows that the μ_{eff} ($\propto (\chi T)^{1/2}$) value decreases with a decrease in temperature.[19] The plot of $1/\chi_m$ versus T follows the Curie–Weiss law with a Weiss constant $\theta = -31.9$ K, which indicates an antiferromagnetic interaction between the paramagnetic Pt_6Rh_2 segments.

Additionally, the single-crystal electrical conductivity of **4** (four probes, direct current) revealed semiconducting character of the material (3.52×10^{-6} S cm^{-1}) at room temperature.[20] Compound **4** shows a typical semiconducting behavior in the temperature range measured (267–295 K), and the activation energy was estimated as 1.0 eV (see Supporting Information).

In summary, the present results demonstrate that the linear chain structure of the amidate-bridged platinum tetramer can be extended to the octameric segment Pt_6Rh_2, which is further extended infinitely by Cl^- bridges. The Pt–Rh bond between the Pt–Rh dimer and the Pt tetramer is the first example of metal–metal bond formed between the tetranuclear platinum chain and any other metal, and suggests that by selecting suitable metal ions the tetranuclear platinum chain can be incorporated into a longer chain by metal–metal bonds. Note, in complex **4** the unpaired electron does not occupy the d_{z^2} orbital of the tetranuclear platinum chain[15] but, different from our expectation, occupies the d_{xy} orbital of the rhodium atom and hops from one rhodium atom to another. This type of long-distance exchange is rare and possibly leads to new electric and magnetic properties. Attempts to prepare a wider variety of heterometallic chain complexes by tailoring the ligands and selecting suitable metals are currently in progress.

Experimental Section

$[Pt_2(PVM)_2(NH_3)_4](PF_6)_2 \cdot H_2O$ (**2**): $NaPF_6$ (0.5 mmol, 0.084 g) was added to a solution of $[Pt(PVM)_2(NH_3)_2] \cdot 2H_2O$ (0.1 mmol, 0.047 g) in MeOH (2 mL). Yellow-green square crystals were obtained after one month (20% yield). Elemental analysis (%) calcd for $C_{20}H_{68}F_{24}N_{12}O_6P_4Pt_4$: C 12.43, H 3.55, N 8.70; found: C 12.58, H 3.34, N 8.08; IR (KBr pellet): $\tilde{\nu}$: C=O stretching, 1622 cm^{-1} (m), 1583 cm^{-1} (s); PF_6^- ion, 841 cm^{-1} (vs).

$[Pt_4(PVM)_4(NH_3)_8](PF_6)_4(ClO_4) \cdot 2H_2O$ (**3**): $AgClO_4$ (2 equiv, 1.0 mmol, 0.207 g) was added to an aqueous solution (2 mL) of *cis*-$[Pt(NH_3)_2Cl_2]$ (0.5 mmol, 0.150 g), and the mixture was stirred for 18 h in the dark. AgCl was then removed by filtration, and the colorless filtrate was warmed at 40 °C for 30 min before the addition of 1 equiv of $[Pt(PVM)_2(NH_3)_2] \cdot 2H_2O$ (0.5 mmol, 0.235 g) and $NaPF_6$ (1.0 mmol, 0.167 g). The mixture was stirred at 40 °C for a further 14 h, then the solution (dark blue) was left to stand for a week before dark blue crystals were separated (61% yield). Elemental analysis (%) calcd for $C_{20}H_{68}ClF_{24}N_{12}O_{10}P_4Pt_4$: C 11.82, H 3.37, N 8.27; found: C 11.89, H 3.27, N 7.73; UV/Vis (KBr pellet): $\lambda_{max} = 621$ nm; IR (KBr pellet): $\tilde{\nu}$: C=O stretching, 1637 cm^{-1} (m), 1583 cm^{-1} (s); ClO_4^- ion, 1097 cm^{-1} (s, br); PF_6^- ion, 843 cm^{-1} (vs).

$\{[PtRh(PVM)_2(NH_3)_2Cl_{2.5}]_2[Pt_2(PVM)_2(NH_3)_4]_2(PF_6)_6 \cdot 2MeOH \cdot 2H_2O\}_n$ (**4**): $RhCl_3 \cdot 3H_2O$ (0.05 mmol; 0.013 g) in MeOH (1 mL) was added to a solution of $[Pt(PVM)_2(NH_3)_2] \cdot 2H_2O$ (0.1 mmol, 0.047 g) and $NaPF_6$ (0.5 mmol, 0.084 g) in MeOH (1 mL). The mixture was placed in a tube for a month. Dark brown crystals formed during this time and were separated, washed with water, and dried (22% yield). Elemental analysis (%) calcd for $C_{42}H_{128}Cl_5F_{36}N_{20}O_{12}P_6Pt_6Rh_2$: C 14.29, H 3.66, N 7.94; found: C 14.07, H 3.57, N 8.16; UV/Vis (KBr pellet): $\lambda_{max} = 475$ nm, 599 nm, 720 nm (sh); IR (KBr pellet): $\tilde{\nu}$: C=O stretching, 1647 cm^{-1} (m), 1566 cm^{-1} (s); PF_6^- ion, 841 cm^{-1} (vs).

Crystal structure determination for **2**–**4**: Measurements were carried out on a Bruker SMART APEX CCD diffractometer equipped with a normal focus Mo-target X-ray tube ($\lambda = 0.71073$ Å) operated at 2000 W power (50 kV, 40 mA) and a CCD two-dimensional detector. A total of 1315 frames were collected with a scan width of 0.3° in ω with an exposure time of 20 (**2**), 40 (**3**), and 60 (**4**) s per frame. The frames were integrated with the SAINT software package with a narrow frame algorithm. Absorption correction was applied by using SADABS. All the structures were solved by direct methods with subsequent difference Fourier syntheses and refinement with the SHELXTL (version 5.1) software package. Non-hydrogen atoms were refined anisotropically, and all hydrogen atoms were placed in the ideal positions.

Crystal data for **2**: $C_{10}H_{20}F_{12}N_6O_3P_2Pt_2$, $M_w = 952.44$, monoclinic, space group $I2/a$, $a = 11.461(4)$, $b = 18.095(6)$, $c = 26.256(10)$ Å, $\beta = 98.543(6)°$, $V = 5385(3)$ Å^3, $Z = 8$, $\rho_{calcd} = 2.350$ g cm^{-3}, $\mu(Mo_{K\alpha}) = 10.605$ mm^{-1}, $F(000) = 3520$, crystal size: $0.60 \times 0.50 \times 0.05$ mm^3, $T = 120$ K; $\lambda(Mo_{K\alpha}) = 0.71073$ Å, $\theta_{min-max} = 1.4$–$27.5°$, total data = 14338, unique data = 5795, $R_{int} = 0.0583$, observed data ($I > 2\sigma(I)$) = 4898, $R = 0.0750$, $R_w = 0.1961$, GOF = 1.066.

Crystal data for **3**: $C_{20}H_{40}ClF_{24}N_{12}O_{10}P_4Pt_4$, $M_w = 2004.33$, triclinic, space group $P\bar{1}$, $a = 14.231(3)$, $b = 14.722(3)$, $c = 15.642(3)$ Å, $\alpha = 75.007(3)$, $\beta = 84.237(3)$, $\gamma = 73.648(4)°$, $V = 3036.3(10)$ Å^3, $Z = 2$, $\rho_{calcd} = 2.192$ g cm^{-3}, $\mu(Mo_{K\alpha}) = 9.457$ mm^{-1}, $F(000) = 1858$, crystal size: $0.50 \times 0.40 \times 0.10$ mm^3, $T = 120$ K; $\lambda(Mo_{K\alpha}) = 0.71073$ Å, $\theta_{min-max} = 2.4$–$26.9°$, total data = 18819, unique data = 12951, $R_{int} = 0.0433$, observed data ($I > 2\sigma(I)$) = 8401, $R = 0.0621$, $R_w = 0.1666$, GOF = 1.055.

Crystal data for **4**: $C_{42}H_{80}Cl_5F_{36}N_{20}O_{12}P_6Pt_6Rh_2$, $M_w = 3480.69$, monoclinic, space group $C2/c$, $a = 24.956(3)$, $b = 12.3284(14)$, $c = 34.205(4)$ Å, $\beta = 106.377(2)°$, $V = 10097(2)$ Å^3, $Z = 4$, $\rho_{calcd} = 2.290$ g cm^{-3}, $\mu(Mo_{K\alpha}) = 8.945$ mm^{-1}, $F(000) = 6500$, crystal size: $0.60 \times 0.05 \times 0.05$ mm^3, $T = 120$ K, $\lambda(Mo_{K\alpha}) = 0.71073$ Å, $\theta_{min-max} = 2.0$–$27.0°$, total data = 30284, unique Data = 11307, $R_{int} = 0.0844$, observed data ($I > 2\sigma(I)$) = 7669, $R = 0.0719$, $R_w = 0.1785$, GOF = 1.037.

For **2**, atoms C4, C8, and F10 were refined isotropically. For **3**, atoms C4, F24, O9, and O10 were found in the final stage, and thus their atom positions were isotropically refined under rigid condition. For **4**, atoms N1, N5, N10, C16, C19, and C20 were refined isotropically. CCDC-265911 (**2**), CCDC-265912 (**3**), and CCDC-265913 (**4**) contain the supplementary crystallographic data for this paper. These data can be obtained free of charge from The Cambridge Crystallographic Data Centre via www.ccdc.cam.ac.uk/data_request/cif.

UV/Vis reflection spectra were recorded on a Shimadzu UV-3101PC spectrophotometer over the range from 400 to 800 nm at room temperature. IR spectra were recorded on a JEOL WINSPEC-50 spectrometer with the samples prepared as KBr pellets. X-band EPR spectra were recorded on a JEOL JES-PX1060 spectrometer at 77 K. Magnetic susceptibility measurements were carried out in the temperature range 2–250 K with a magnetometer MPMS-7 (Quantum Design) equipped with a SQUID sensor.

Received: March 23, 2005
Published online: July 25, 2005

Keywords: chain structures · mixed-valent compounds · platinum · rhodium

[1] J. S. Miller, *Extended Linear Chain Compounds*, *Vols. 1–3*, **1982**, Plenum, New York.

[2] a) J. K. Bera, K. R. Dunbar, *Angew. Chem.* **2002**, *114*, 4633; *Angew. Chem. Int. Ed.* **2002**, *41*, 4453; b) H. Kitagawa, T. Mitani, *Coord. Chem. Rev.* **1999**, *190–192*, 1169.

[3] J. S. Miller, A. J. Epstein, *Synthesis and Properties of Low-Dimensional Materials*, The New York Academy of Science, New York, **1978**.

[4] For recent reports on infinite 1D chains, see: a) G. M. Finniss, E. Canadell, C. Campana, K. R. Dunbar, *Angew. Chem.* **1996**, *108*, 2946; *Angew. Chem. Int. Ed. Engl.* **1996**, *35*, 2772; b) M. E. Prater, L. E. Pence, R. Clerac, G. M. Finniss, C. Campana, P. Auban-Senzier, D. Jerome, E. Canadell, K. R. Dunbar, *J. Am. Chem. Soc.* **1999**, *121*, 8005; c) K. Sakai, M. Takeshita, Y. Tanaka, T. Ue, M. Yanagisawa, M. Kosaka, T. Tsubomura, M. Ato, T. Nakano, *J. Am. Chem. Soc.* **1998**, *120*, 11353; d) H. Kitagawa, N. Onodera, T. Sonoyama, M. Yamamoto, T. Fukawa, T. Mitani, M. Seto, Y. Maeda, *J. Am. Chem. Soc.* **1999**, *121*, 10068; e) F. A. Cotton, E. V. Dikarev, M. A. Petrukhina, *J. Organomet. Chem.* **2000**, *596*, 130; f) F. A. Cotton, E. V. Dikarev, M. A. Petrukhina, *J. Chem. Soc. Dalton Trans.* **2000**, 4241; g) F. P. Pruchnik, P. Jakimowicz, Z. Ciunik, *Inorg. Chem. Commun.* **2001**, *4*, 726; h) K. Sakai, E. Ishigami, Y. Konno, T. Kajiwara, T. Ito, *J. Am. Chem. Soc.* **2002**, *124*, 12088; i) M. Mitsumi, S. Umebayashi, Y. Ozawa, M. Tadokoro, H. Kawamura, K. Toriumi, *Chem. Lett.* **2004**, *33*, 970; j) M. Yamashita, D. Kawakami, S. Matsunaga, Y. Nakayama, M. Sasaki, S. Takaishi, F. Iwahori, H. Miyasaka, K. Sugiura, Y. Wada, H. Miyamae, H. Matsuzaki, H. Okamoto, H. Tanaka, K. Marumoto, S. Kuroda, *Angew. Chem.* **2004**, *116*, 4867; *Angew. Chem. Int. Ed.* **2004**, *43*, 4763.

[5] a) C. Tejel, M. A. Ciriano, L. A. Oro, *Chem. Eur. J.* **1999**, *5*, 1131; b) K. Matsumoto, K. Sakai, *Adv. Inorg. Chem.* **2000**, *49*, 375.

[6] For tetranuclear $Pt^{2.25+}$ chains (platinum blue), see: a) J. K. Barton, H. N. Rabinowitz, D. J. Szalda, S. J. Lippard, *J. Am. Chem. Soc.* **1977**, *99*, 2827; b) J. K. Barton, D. J. Szalda, H. N. Rabinowitz, J. V. Waszczak, S. J. Lippard, *J. Am. Chem. Soc.* **1979**, *101*, 1434; c) T. V. O'Halloran, M. M. Roberts, S. J. Lippard, *J. Am. Chem. Soc.* **1984**, *106*, 6427; d) P. K. Mascharak, I. D. Williams, S. J. Lippard, *J. Am. Chem. Soc.* **1984**, *106*, 6428; e) K. Matsumoto, J. Matsunami, H. Urata, *Chem. Lett.* **1993**, 597; f) K. Sakai, Y. Tanaka, Y. Tsuchiya, K. Hirata, T. Tsubomura, S. Iijima, A. Bhattacharjee, *J. Am. Chem. Soc.* **1998**, *120*, 8366.

[7] a) W. Chen, K. Matsumoto, *Inorg. Chim. Acta* **2003**, *342*, 88; b) W. Chen, F. Liu, T. Nishioka, K. Matsumoto, *Eur. J. Inorg. Chem.* **2003**, 4234.

[8] a) A. Erxleben, I. Mutikainen, B. Lippert, *J. Chem. Soc. Dalton Trans.* **1994**, 3667; b) E. Zangrando, F. Pichierri, L. Randaccio, B. Lippert, *Coord. Chem. Rev.* **1996**, *156*, 275.

[9] K. Uemura, K. Matsumoto, unpublished results.

[10] For selected Pt–Rh dimers with other ligands, see: a) R. R. Guimerans, F. E. Wood, A. L. Balch, *Inorg. Chem.* **1984**, *23*, 1307; b) A. L. Balch, R. R. Guimerans, J. Linehan, F. E. Wood, *Inorg. Chem.* **1985**, *24*, 2021; c) A. L. Balch, V. J. Catalan, *Inorg. Chem.* **1992**, *31*, 3934.

[11] The dimerization process of **1** was monitored by ^{1}H NMR spectroscopy and ESI-MS (see Supporting Information).

[12] For tetranuclear Pt^{2+} chains, see: a) L. S. Hollis, S. J. Lippard, *J. Am. Chem. Soc.* **1981**, *103*, 1230; b) J.-P. Laurent, P. Lepage, F. Dahan, *J. Am. Chem. Soc.* **1982**, *104*, 7335; c) L. S. Hollis, S. J. Lippard, *Inorg. Chem.* **1983**, *22*, 2600; d) L. S. Hollis, S. J. Lippard, *J. Am. Chem. Soc.* **1983**, *105*, 3494; e) K. Matsumoto, H. Miyamae, H. Moriyama, *Inorg. Chem.* **1989**, *28*, 2959.

[13] For tetranuclear $Pt^{2.5+}$ chains (platinum tan), see: a) K. Matsumoto, K. Fuwa, *J. Am. Chem. Soc.* **1982**, *104*, 897; b) K. Matsumoto, H. Takahashi, K. Fuwa, *Inorg. Chem.* **1983**, *22*, 4086.

[14] a) K. Sakai, K. Matsumoto, *J. Am. Chem. Soc.* **1989**, *111*, 3074; b) K. Matsumoto, K. Sakai, K. Nishio, Y. Tokisue, R. Ito, T. Nishide, Y. Shichi, *J. Am. Chem. Soc.* **1992**, *114*, 8110.

[15] a) J. K. Barton, C. Caravana, S. J. Lippard, *J. Am. Chem. Soc.* **1979**, *101*, 7269; b) P. Arrizabalaga, P. Castan, M. Geoffroy, J.-P. Laurent, *Inorg. Chem.* **1985**, *24*, 3656.

[16] F. Mehran, B. A. Scott, *Phys. Rev. Lett.* **1973**, *31*, 99.

[17] F. Mehran, B. A. Scott, *Phys. Rev. Lett.* **1973**, *31*, 1347.

[18] A. G. Bunn, B. B. Wayland, *J. Am. Chem. Soc.* **1992**, *114*, 6917.

[19] See Supporting Information for the magnetic measurements of **4**.

[20] Only the electrical conductivity perpendicular to the chain direction was measured. It was impossible to measure the conductivity parallel to the chain, as the crystal is a thin plate (see Supporting Information).

